IOP Publishing Physica Scripta
Phys. Scr. 95 (2020) 045214 (8pp) https://doi.org/10.1088/1402-4896/ab635c

Localized solitary waves and their dynamical stabilities in magnetized dusty plasma

Lin Song[1,2], Juan Zhang[1,2], Zhikun Zhou[1,2], Xiaohuan Wan[1,2], Xiaolin Li[1,2], Na Tang[1,2], Xueying Yang[1,2] and Yuren Shi[1,2]

[1] College of Physics and Electronic Engineering, Northwest Normal University, Lanzhou 730070, People's Republic of China
[2] Laboratory of Atomic Molecular Physics and Functional Material, Northwest Normal University, Lanzhou 730070, People's Republic of China

E-mail: shiyr@nwnu.edu.cn

Received 16 October 2019, revised 17 December 2019
Accepted for publication 18 December 2019
Published 14 February 2020

Abstract

We consider a magnetized dusty plasma, which composed of low-temperature and high-temperature ions, electrons, and dust particles. The dynamical behaviors can be described by a (3+1)-dimensional Zakharov–Kuznetsov equation (ZKE). Interestingly, a type of completely localized solitary waves, which are different from the line solitons, of ZKE are obtained analytically and approximately for the first time. This kind of solitary wave is also confirmed numerically by the Petviashvili method. Both the analytical and numerical results indicate that the amplitude of the localized wave is proportional to its velocity and inverse proportional to the nonlinear interaction strength. A finite difference scheme with second-order accuracy is presented to make the long-time nonlinear evolution of ZKE. The numerical results indicate that the localized solitons are always dynamically stable. Moreover, the collision between two solitary waves is investigated numerically. The results show that both elastic and inelastic collision exist when two localized solitary waves colliding.

Keywords: magnetized dusty plasma, solitary wave, dynamical stability, Petviashvili method

(Some figures may appear in colour only in the online journal)

1. Introduction

It is accepted that most matter in the Universe is in the plasma state, in which the dust is a omnipresent ingredient. Dusty plasmas are the ionized gases containing small particles of solid matter since they discovered in laboratory and in space [1, 2]. It has wide applications in the fields of laboratories, industrial plasma processing, and astrophysics [3–6]. Thus, the study of dust plasma physics has became a new branch of physics at the end of last century [2, 7]. There are many research subjects in the frontier of dust plasma [8–14]. Among them, one of the popular subjects in dusty plasmas is studying the linear and nonlinear waves. Nonlinear wave theory is applied in a variety of physical systems, such as ordinary metals, semiconductors, super dense astrophysical environments, nano-devices, and in laser-plasma experiments [15–18], nonlinear hydroelastic waves, biologically-inspired pumping systems, thermoelasticity in dipolar materials [19–21], and so on. Many researchers are interested in the study of nonlinear waves. Dusty plasma supports mainly two types of acoustic waves, respectively, high frequency dust ion acoustic waves (DIAWs) involving mobile ions and static dust grains, and a low frequency dust acoustic waves (DAWs) involving mobile dust grains [22, 23]. More than a decade ago, Rao, Shukla, and Yu [24] predicted the existence of nonlinear DAWs in an unmagnetized dusty plasma for the first time. The existence of DIAWs was predicted by Shukla and Silin [25]. Both the DIAWs and the DAWs have been observed in the Earth's lower-ionospheric regions as well as in many laboratory experiment [26].

The Zakharov–Kuznetsov equation (ZKE) can be used to describe the small but finite amplitude DAWs in a magnetized two-ion-temperature dusty plasma with dust size distribution [27]. [28] also obtained the ZKE for weakly nonlinear ion-acoustic waves in a strongly magnetized lossless plasma in two dimensions. In addition, a class of traveling wave solutions for the electric field potential, electric field and magnetic field of the ZKE have been presented. In [29], the authors

considered a 3D dusty plasma system which consists of massive, negatively charged dust fluid in the presence of an external static magnetic field. They found that the 3D ZKE can also be employed to describe the time-evolution of dust-acoustic solitary waves in such a nonlinear system. In particular, a finite difference scheme was established to study the transverse instability of the line solitons. The numerical results indicate that a localized solitary wave will be formed when the line soliton is unstable. However, by our best knowledge, most work is focused on the transverse stability of line solitons [30] and less work has been done on the properties of the localized wave. Strictly speaking, the line soliton is not completely localized.

In this paper, we consider a magnetized dusty plasma, which composed of low-temperature and high-temperature ions, electrons, and dust particles. The dynamical behaviors is assumed to be described by a 3D ZKE. Interestingly, a type of completely localized solitary waves, which are different from the line solitons, are obtained analytically and approximately for the first time. This kind of solitary wave is also confirmed numerically by the Petviashvili method. Both the analytical and numerical results indicate that the amplitude of the localized wave is proportional to its velocity and inverse proportional to the nonlinear interaction strength. A finite difference scheme with second-order accuracy is presented to make the long-time nonlinear evolution. The numerical results exhibit that the localized solitons are always dynamically stable. Moreover, the collision between two solitary waves is investigated numerically. The results show that both elastic and inelastic collision exist when two localized solitary waves colliding.

2. The localized solitary wave solution of ZKE

When a magnetized dusty plasma system composed of low-temperature and high-temperature ions, electrons, and dust particles with a large amount of negative charge is considered, by using the reductive perturbation method, the 3D ZKE is again obtained, which reads [27]

$$\frac{\partial\phi_1}{\partial t}+\alpha\phi_1\frac{\partial\phi_1}{\partial\xi}+\beta\frac{\partial^3\phi_1}{\partial\xi^3}+\gamma\frac{\partial}{\partial\xi}\left(\frac{\partial^2\phi_1}{\partial\eta^2}+\frac{\partial^2\phi_1}{\partial\zeta^2}\right)=0 \tag{1}$$

with α denotes the nonlinear strength, β and γ are the dispersion coefficients, and $\alpha=-\frac{3Z_d^2}{2v_0^3m_d^2}-\frac{v_0^2}{2}s^2(\beta_1^2\nu-\mu_l-\beta_2^2\mu_h)$, $\beta=\frac{v_0}{2}$, $\gamma=\frac{v_0}{2}\left(1+\frac{m_d}{\omega_{cd}^2}\right)$, where all the physical quantities are dimensionless. Here, v_0 is the linear dust acoustic velocity, $\beta_1=T_{il}/T_e$, $\beta_2=T_{ih}/T_e$. T_{il}, T_{ih}, T_e denote the temperature of low temperature ions, high temperature ions and electrons, respectively. $\mu_l=n_{il0}/Z_{d0}n_{d0}$, $\mu_h=n_{ih0}/Z_{d0}n_{d0}$, Z_{d0} is the number of charges on undisturbed dust particles. n_{d0}, n_{il0}, n_{ih0} are respectively the undisturbed number density of dust particles, low temperature ions and high temperature ions. The physical meaning of other symbols are the same as in [27]. For a typical dusty plasma [31, 32], the dimension quantities read $n_{e0}\sim n_{i0}\sim 10^8\,\mathrm{cm}^{-3}$, $n_{d0}\sim 10^4\,\mathrm{cm}^{-3}$, $T_{il}\sim T_{ih}\sim 2.5\,\mathrm{eV}$, $T_e\sim 0.025\,\mathrm{eV}$, $Z_d\sim 1000$, $m_d\sim 1.74\times 10^{-5}\,\mathrm{kg}$. One then can get $\alpha\approx 1\,167.93$. For another typical dusty plasma [33], $n_{e0}\sim n_{i0}\sim 10^5\,\mathrm{cm}^{-3}$, $n_{d0}\sim 10^5\,\mathrm{cm}^{-3}$, $T_e\sim T_i\sim 0.1\,\mathrm{eV}$, $Z_d\sim 10$, $m_d\sim 10^{-9}\,\mathrm{kg}$, one can obtain $\alpha\approx -501.74$. We see that the nonlinear strength α can be both positive and negative, implying that both bright solitons and dark solitons can exist in such a nonlinear system. For convenient, in the following, we only consider the two-dimensional case. Thus, we have $\frac{\partial}{\partial\zeta}=0$. Then equation (1) becomes

$$\frac{\partial\phi_1}{\partial t}+\alpha\phi_1\frac{\partial\phi_1}{\partial\xi}+\beta\frac{\partial^3\phi_1}{\partial\xi^3}+\gamma\frac{\partial^3\phi_1}{\partial\xi\partial\eta^2}=0. \tag{2}$$

We now try to seek the localized solitary waves observed in [27] analytical and approximately. Suppose that the wave propagates along ξ direction with velocity c, then one can make the traveling wave transformation

$$\phi_1(\xi,\eta,t)=u(x,y),\ x=\xi-ct,\ y=\eta.$$

After which, equation (2) can be translated to

$$-cu+\frac{1}{2}\alpha u^2+\beta\frac{\partial^2u}{\partial x^2}+\gamma\frac{\partial^2u}{\partial y^2}=0. \tag{3}$$

Here, the integration constant is set to be zero because of locality. Assuming that the localized wave is a Gaussian profile one, then it can be expressed as

$$u=A\exp\left[-\frac{(x-x_0)^2+B(y-y_0)^2}{W}\right], \tag{4}$$

where A and W ($W>0$) is the amplitude and width of the wave, respectively. B is a positive constant. Both of them will be determined later. (x_0, y_0) is the center position of the wave and it can be arbitrary. Note that, in general, equation (4) is not an exact solution of equation (3). Substituting equation (4) into the left hand of equation (3) yields the residual error

$$\epsilon=\frac{1}{2}A\mathcal{G}\left(\alpha A\mathcal{G}-2c+\frac{8B^2\gamma(y-y0)^2-4W(\beta+B\gamma)+8\beta(x-x0)^2}{W^2}\right) \tag{5}$$

with $\mathcal{G}=\exp\left[-\frac{(x-x_0)^2+B(y-y_0)^2}{W}\right]$. One can see that equation (4) may be an exact solution to equation (3) if $\epsilon\equiv 0$. However, unfortunately, this is not the case because equation (4) is only an approximated one. We then think that the smaller the ε is, the better the u is. A natural choice is to minimize the magnitude of ε, which can be measured by its 2-norm $\|\varepsilon\|_2=\sqrt{\int\varepsilon^2\mathrm{d}x\mathrm{d}y}$.

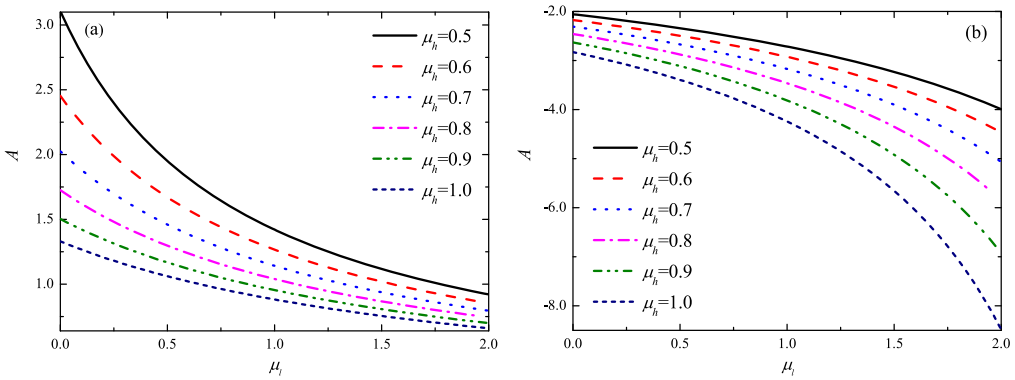

Figure 1. Amplitudes of the localized solitary waves, given by equation (7), change with μ_l under different μ_h. (a) $Z_d = 2.0$, $m_d = 1.5$, $\beta_1 = 0.1$, $v_0 = 1.8$ (b) $Z_d = 1.0$, $m_d = 1.0$, $\beta_1 = 1.5$, $v_0 = 1.0$. Other parameters are taken as $s = 1.0$, $c = 1.0$, $\beta_2 = 1.5$, $\nu = 1.0$.

For the sake of simplicity, we minimize $\|\varepsilon\|_2^2$ instead of $\|\varepsilon\|_2$, just as the least square method does. Then we have

$$\frac{\partial\|\varepsilon\|_2^2}{\partial A} = 0, \frac{\partial\|\varepsilon\|_2^2}{\partial W} = 0, \frac{\partial\|\varepsilon\|_2^2}{\partial B} = 0. \tag{6}$$

Although equation (6) can be solved exactly, but the expressions are rather lengthy. A relatively easy way is to solve it in a semi-numerical manner, which can be performed easily in **Mathematica** software by the **NSolve** command. The results read

$$\begin{aligned} A &= \frac{4.242\,505c}{\alpha}, B = \frac{\beta}{\gamma}, W = \frac{4.356\,485\beta}{c}, \\ \|\varepsilon\|_2^2 &= \frac{3.688\,285c^3\beta\sqrt{\gamma}}{\alpha^2\sqrt{\beta}} \end{aligned} \tag{7}$$

The solitary wave given by equation (4) is completely localized because it satisfies $u(\pm\infty, y) = u(x, \pm\infty) = 0$. Now we take a deeply analysis on its properties based upon equations (4) and (7). Both W, B and $\|\varepsilon\|_2^2$ are positive leads to

$$\mathrm{sgn}(c) = \mathrm{sgn}(\beta) = \mathrm{sgn}(\gamma),$$

where $\mathrm{sgn}(x)$ is the sign function. If $\beta > 0$, then one has $c > 0$, suggesting that the solitary wave propagates along ξ direction under this situation. While it travels along $-\xi$ direction when $\beta < 0$. Therefore, the wave propagating direction is totaly determined by β. The amplitude of the solitary wave, i.e. A, is proportional to its velocity c and inverse proportional to nonlinear strength α, implying that a faster wave has larger peak than a lower one. This property is similar to the KdV soliton. If α and c have the same sign, then $A > 0$ and equation (4) represents a bright soliton. On the contrary, equation (4) is a dark soliton when c and α have different sign. We know that α can be both positive or negative in experiments, so both bright solitons and dark solitons can be excited in such a nonlinear system. From the expression of $\|\varepsilon\|_2^2$, it is obviously that $\|\varepsilon\|_2^2$ is proportional to c^3 when other parameters are fixed, implying that this localized solution is appropriate only when $|c|$ is small enough.

In ZKE (1), all the physical parameters, such as the linear acoustic velocity, effective temperature, dust particle mass and charge number and so on, are absorbed in the nonlinear coefficient α. So a fixed α corresponds various combination of other parameters. For a typical plasma, the parameters read μ_l, $\mu_h \sim 0.1$–1000, β_1, $\beta_2 \sim 0.1$–2 [33]. To see it more clearly, figure 1 depicts the change for the amplitude A of solitary waves, given by equation (7), with respect to μ_l under different μ_h. From figure 1(a), it is obviously that A decreases as μ_l increases. Especially, it decreases rapidly when μ_l is near zero. For a fixed μ_l, it can also be noted that A decreases when μ_h increases. In figure 1(a), A is always positive, indicating that all the localized solitary waves are bright solitons under these parameters. Figure 1(b) displays another case that A is always negative, i.e. the localized solitary waves are dark solitons. Note that the amplitude of the soliton should be regarded as $|A|$ with this situation. We see from figure 1(b) that A decreases as μ_l increases, which means the amplitude of dark solitons increases as μ_l increases. This is differ from the case in figure 1(a), where the amplitude of bright solitons decreases when μ_l increases.

Figure 2 shows the change for A versus β_1 with different β_2. One can easily see that both in figures 2(a) and (b), A increases as β_1 increases when other parameters are fixed. However, A is always positive in figure 2(a), while it is negative in figure 2(b). Therefore, the solitons are bright soliton in figure 2(a) and dark soliton in figure 2(b). We can come to the conclusion that the amplitude of bright (dark) soliton increases (decreases) when β_1 increases. In experiments, one can observe the bright soliton or dark soliton via adjusting the physical parameters, such as μ_h, μ_l, β_1, β_2, and so on.

Solution (4) is no longer valid when $|c|$ is not small. Then we can numerically find the localized solitary waves by the Petviashvili method [34–36]. This method is an effective numerical method for calculating localized solitary waves to many nonlinear problems in modern mathematical physics. Convergence conditions for constant-coefficient equations with power-law nonlinearity were obtained by Pelinovsky and Stepanyants. This approach is also extended to solve more general wave equations. It often converges faster than other methods [36] and is easy to implement in **Matlab**. Now we apply the Petviashvili method to seek the localized solitary waves of ZKE (2) by solving equation (3). For the sake of simplicity and without loss of generality, we take $\gamma = \beta$. If it

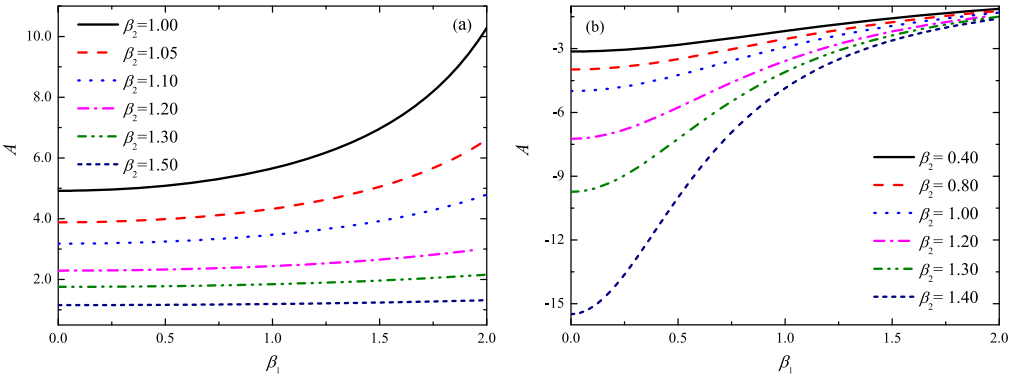

Figure 2. Amplitudes of the localized solitary waves, given by equation (7),change with β_1 under different β_2. (a) $s = 1.5$, $\mu_h = 2$, $\nu = 0.1$ (b) $s = 1.0$, $\mu_h = 1.2$, $\nu = 1.2$. Other parameters are taken as $Z_d = 1.0$, $m_d = 1.0$, $c = 1.0$, $v_0 = 1.0$, $\mu_l = 0.1$.

is not so, this can be achieved by mathematical transformation $\tilde{\eta} = \sqrt{\frac{\beta}{\gamma}}\eta$.

Apply the 2D Fourier transformation on both sides in equation (3), one can obtain

$$u = \mathcal{F}^{-1}\left[\frac{\frac{1}{2}\alpha\mathcal{F}[u^2]}{c + \beta(k_x^2 + k_y^2)}\right], \tag{8}$$

where $\mathcal{F}[\bullet]$ and $\mathcal{F}^{-1}[\bullet]$ represents the 2D Fourier transformation and inverse Fourier transformation, respectively. They are defined as

$$\mathcal{F}[f(\vec{r})] = \int f(\vec{r})\mathrm{e}^{-\mathrm{i}\vec{k}\cdot\vec{r}}\mathrm{d}\vec{r},$$
$$\mathcal{F}^{-1}[F(\vec{k})] = \frac{1}{2\pi}\int F(\vec{k})\mathrm{e}^{\mathrm{i}\vec{k}\cdot\vec{r}}\mathrm{d}\vec{k}$$

with $\vec{r} = (x, y)$, $\vec{k} = (k_x, k_y)$. From equation (8), an iteration equation can be established

$$u_{n+1} = \mathcal{F}^{-1}\left[\frac{\frac{1}{2}\alpha\mathcal{F}[u_n^2]}{c + \beta(k_x^2 + k_y^2)}\right], n = 0, 1, 2,\ldots, \tag{9}$$

where n is the iteration index. However, this iteration is generally divergent or converges to the trivial solution $u \equiv 0$. To overcome this trouble, introducing the stability factor

$$S_n = \frac{\langle cu_n - \beta\nabla^2 u_n, u_n\rangle}{\left\langle\frac{1}{2}\alpha u_n^2, u_n\right\rangle}.$$

Here, ∇^2 is the 2D Laplacian operator. The inner product for two functions $f(\vec{r})$ and $g(\vec{r})$ is defined as $\langle f, g\rangle = \int f(\vec{r})g^*(\vec{r})\mathrm{d}\vec{r}$, '*' denotes the complex conjugate. Then the iteration equation (9) is rewritten as

$$u_{n+1} = S_n^2\mathcal{F}^{-1}\left[\frac{\frac{1}{2}\alpha\mathcal{F}[u_n^2]}{c + \beta(k_x^2 + k_y^2)}\right], n = 0, 1, 2,\ldots. \tag{10}$$

It is worthy remarkable that c must has the same sign as β to eliminate the singularity of equation (10). Thus we have sgn(c) = sgn(β) again, just as before.

As an example, figure 3(a) shows the profile of a bright soliton for $\alpha = 6$, $\beta = 3$, $c = 1$ and figure 3(b) illustrates a dark soliton when $\alpha = 6$, $\beta = -3$, $c = -1$. Both the bright soliton and dark soliton are obtained by the above Petviashvili method. We noticed that it converges to the wanted results rapidly, even if $|c|$ is large. The initial condition for iterating is taken as the analytical and approximated solution given before. The computation domain is set to be $x, y \in [-30, 30]$ and the grids numbers are $N_x = N_y = 512$. When $|c|$ is small or β is large, the computation domain should be enlarged because the soliton becomes 'fatter'.

Figure 4 displays how the amplitude of localized solitary wave varies with its velocity c or nonlinear strength α when β is fixed. We find that A increases as c increases (see figure 4(a)) and A is proportional to its velocity c if α is given, implying that a faster soliton has larger amplitude than a slower one. In figure 4(b), it can be seen easily that A decrease as α increases when c is given. Heuristically, from equation (7), one can guess that maybe A is inverse proportional to α. This is indeed the case. To see this more clearly, in figure 4(b), the black line shows a inverse proportional function expressed as $A = 23.919\,564/\alpha$ for $c = 5$, which is nearly same as the numerical result. All these results agree qualitatively with the analytical results given by equation (7). However, for quantitative, it is also noted that the analytical result is less than corresponding numerical result. Further computation shows that A does not depend on the dispersion coefficient β. But β affects the width of soliton, as shown in equation (7).

3. Nonlinear dynamic stability and collision of localized solitary waves

Now we numerically investigate the nonlinear dynamic stability of the localized solitary waves given by the Petviashvili method in previous section. At the initial time $t = 0$, a white noise is

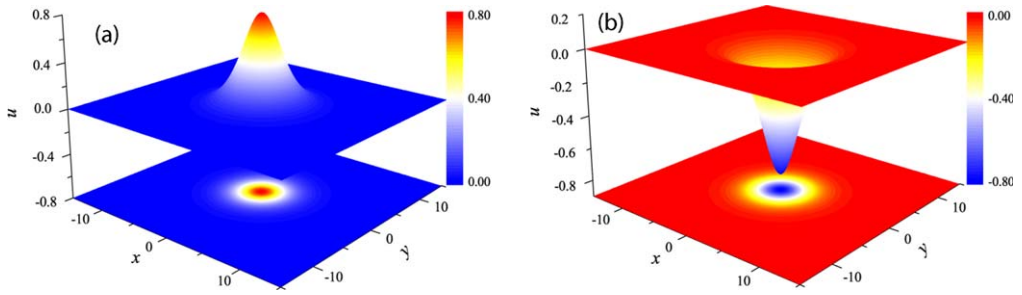

Figure 3. Profiles of localized solitary waves of 2D ZKE. (a) bright soliton ($\alpha = 6, \beta = 3, c = 1$) (b) dark soliton ($\alpha = 6, \beta = -3, c = -1$).

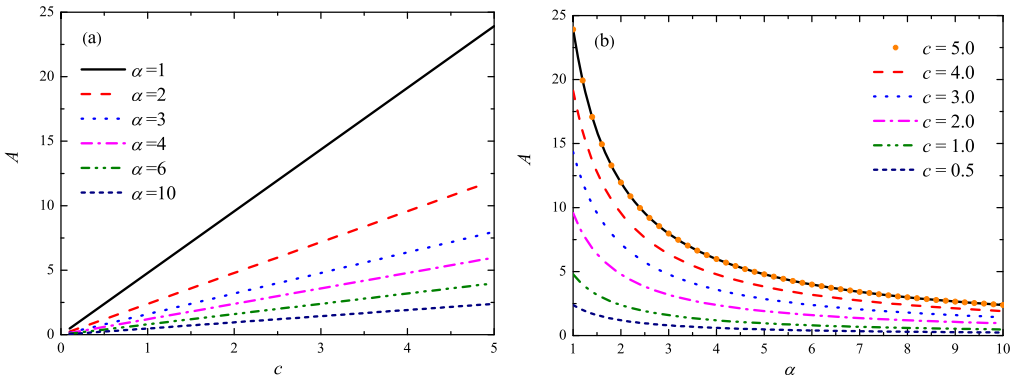

Figure 4. Amplitude of the localized solitary wave of 2D ZKE ($\beta = 3$) (a) A versus c when α is fixed (b) A versus α when c is fixed.

added to the wave. One can explore the stability by observing the long-time evolution of the disturbed solitary wave. If the amplitude of the soliton does not vary significantly, and the wave profile can be held well, then the solitary wave is dynamically stable. Otherwise, it is dynamically unstable.

Firstly, we present a finite difference scheme for time-evolution of 2D ZKE (2)

$$\begin{aligned}&\frac{1}{\Delta t}\delta_t\phi^n_{1,j,p} + \frac{\alpha}{8\Delta\xi}(\phi^{n+1}_{1,j,p} + \phi^n_{1,j,p})\delta_\xi(\phi^{n+1}_{1,j,p} + \phi^n_{1,j,p})\\ &+ \frac{\beta}{4\Delta\xi^3}\delta^3_\xi(\phi^{n+1}_{1,j,p} + \phi^n_{1,j,p})\\ &+ \frac{\gamma}{4\Delta\xi\Delta\eta^2}\delta^2_\eta\delta_\xi(\phi^{n+1}_{1,j,p} + \phi^n_{1,j,p}) = 0,\end{aligned} \tag{11}$$

where

$$\begin{aligned}\delta_t\phi^n_{1,j,p} &= \phi^{n+1}_{1,j,p} - \phi^n_{1,j,p},\\ \delta_\xi\phi^n_{1,j,p} &= \phi^n_{1,j\ +\ 1,p} - \phi^n_{1,j-1,p}\\ \delta^3_\xi\phi^n_{1,j,p} &= \phi^n_{1,j\ +\ 2,p} - 2\phi^n_{1,j+1,p}\\ &\quad + 2\phi^n_{1,j-1,p} - \phi^n_{1,j-2,p}\\ \delta^2_\eta\delta_\xi\phi^n_{1,j,p} &= \phi^n_{1,j+1,p+1} - 2\phi^n_{1,j+1,p}\\ &\quad + \phi^n_{1,j+1,p-1} - \phi^n_{1,j-1,p+1}\\ &\quad + 2\phi^n_{1,j-1,p} - \phi^n_{1,j-1,p-1}\end{aligned}$$

Δt is the temporal step and $\Delta\xi$, $\Delta\eta$ is spatial step along ξ and η directions, respectively. $\phi^n_{1,jp}$ represents the numerical value of $\phi_1(\xi_j, \eta_p, t_n)$ in node (j, p, n) at nth layer. The numerical scheme (11) is a two-layer implicit one and its truncation error reads

$$\begin{aligned}T(\xi_j, \eta_p, t_n) = &\frac{1}{12}[2\phi_{1,ttt} + 3\alpha\phi_{1,tt}\phi_{1,\xi} + 3\alpha\phi_{1,t}\phi_{1,\xi,t}\\ &+ 3\alpha\phi_1\phi_{1,tt\xi} + 3\beta\phi_{1,tt\xi\xi\xi} + 3\gamma\phi_{1,tt\xi\eta\eta}]^n_{j,p}\Delta t^2\\ &+ O(\Delta t^4) + \frac{1}{12}[2\alpha\phi_1\phi_{1,\xi\xi\xi} + 3\beta\phi_{1,\xi\xi\xi\xi\xi}\\ &+ 2\gamma\phi_{1,\xi\xi\xi\eta\eta}]^n_{j,p}\Delta\xi^2 + O(\Delta\xi^4)\\ &+ \frac{1}{12}\gamma\phi_{1,\xi\eta\eta\eta\eta}|^n_{j,p}\ \Delta\eta^2 + O(\Delta\eta^4)\\ =\ &O(\Delta t^2 + \Delta\xi^2 + \Delta\eta^2).\end{aligned} \tag{12}$$

Therefore, this scheme is a second-order accuracy one. The numerical stability can be analyzed approximately by the so-called 'coefficient-frozen' method [37]. Let $\phi^{n+1}_{1,j,p} + \phi^n_{1,j,p}$ be a constant σ, and suppose $\phi^n_{1,j,p} = V^n e^{iq_\xi j\Delta\xi}e^{iq_\eta p\Delta\eta}$, where q_ξ and q_η are arbitrary real numbers. Then one can get the error growth factor $G = \frac{1+ig}{1-ig}$, where

$$g = \frac{4\beta\Delta tC_\xi S^3_\xi}{\Delta\xi^3} - \frac{\alpha\sigma\Delta tC_\xi S_\xi}{2\Delta\xi} + \frac{4\gamma\Delta tC_\xi S_\xi S^2_\eta}{\Delta\xi\Delta\eta^2}$$

$$C_\xi = \cos\left(\frac{q_\xi\Delta\xi}{2}\right),\ S_\kappa = \sin\left(\frac{q_\kappa\Delta\kappa}{2}\right),\ (\kappa = \xi, \eta).$$

Thus, the numerical scheme is absolutely stable because of $|G|^2 \equiv 1$. When the numerical method is performed (The **Matlab** software is employed.), periodic boundary conditions are used in both ξ and η directions.

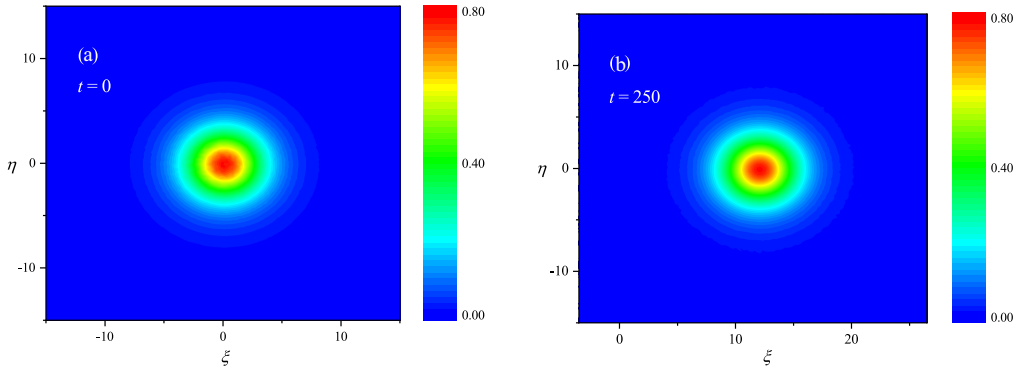

Figure 5. Contour plots of the wave profiles under disturbance at $t = 0$ and $t = 250$.

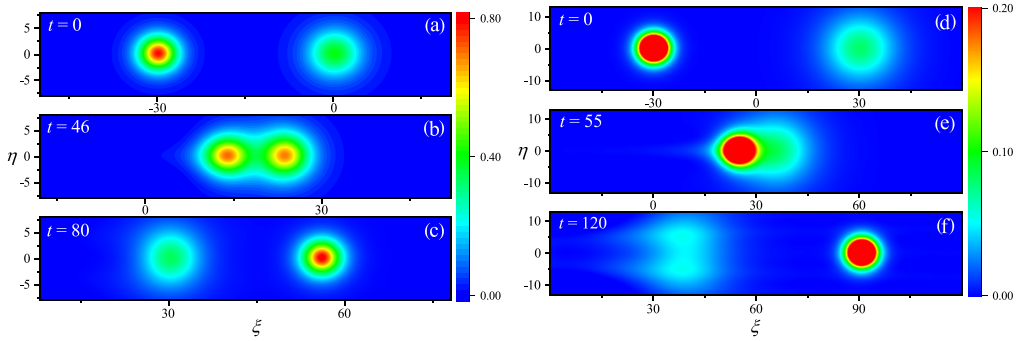

Figure 6. Collision of two localized solitary waves described by the 2D ZKE ($\alpha = 6$, $\beta = 3$, $c_1 = 1$, $\xi_{1,0} = -30$). (a,b,c) $c_2 = 0.5$, $\xi_{2,0} = 0$ (d,e,f) $c_2 = 0.1$, $\xi_{2,0} = 30$.

Figures 5(a) and (b) is the contour plot of a disturbed localized solitary wave at time $t = 0$ and $t = 250$, respectively, for $\alpha = 6$, $\beta = 3$, $c = 1$. At initial time $t = 0$, the soliton is perturbed by adding a white noise, with amplitude 0.01. The wave profile is displayed in figure 5(a). Figure 5(b) illustrates the soliton profile after a long-time evolution by the numerical scheme (11). One can see that the wave shape is kept well after long enough time. The numerical result also indicate that the amplitude of the wave is nearly invariant, suggesting that the localized solitary wave is dynamically stable. The computation domain is set to be $\xi \in [-30, 30]$, $\eta \in [-15, 15]$ and the grids numbers are $N_\xi = 256$, $N_\eta = 128$. The temporal step is taken as $\Delta t = 0.0001$.

We also numerically investigated the nonlinear stability of the localized solitary wave under many other parameters. All the numerical results declare that the wave is dynamically stable. Therefore, this type of soliton has strong anti-interference capability.

Wave collision is a very popular phenomenon in plasma. There are two kinds of collision between two waves. One is the waves propagate with opposite direction, which is called head-on collision; the other is that the waves propagate in the same direction, which is called catching up with collision. Due to the previous numerical results, the localized solitary waves described by the 2D ZKE are always dynamically stable. Now we numerically investigate the collision between two localized solitary waves. Because the parameter β is already fixed for a given ZKE, thus the two solitons must propagate along the same direction, which leads the collision is the so-called 'catching up with collision'. At initial time $t = 0$, these two solitons, which are given by the Petviashvili method, are placed apart from each other. Without loss of generality, the soliton with higher amplitude (named soliton 1) is placed at position ($\xi_{0,1}$,0) and another with lower amplitude (named soliton 2) is placed at position ($\xi_{0,2}$,0) ($\xi_{0,1} < \xi_{0,2}$). They are far enough with each other. The amplitude and velocity of soliton 1 (soliton 2) is denoted by A_1 (A_2) and c_1 (c_2), respectively. The computation domain is set to be $\xi \in [-120, 120]$, $\eta \in [-60, 60]$ and the grids numbers are $N_\xi = 512$, $N_\eta = 256$. The temporal step is adopted as $\Delta t = 0.001$.

Figures 6(a)–(c) are contour plots at different time for the collision of two solitary waves, where the difference between their amplitudes is not too large ($A_1/A_2 = 2$). Soliton 1 gradually catches up with soliton 2 and collides. Then passes soliton 2 until they separate again. Radiation with very small amplitude will be excited during collision. When the collision finished, both the amplitude, velocity and waveform of two solitons are approximately restored as before. Therefore, this type of collision can be regarded as the elastic collision.

Figures 6(d)–(f) depict the collision process of another two solitary waves, where the difference between their amplitudes is large ($A_1/A_2 = 10$). Soliton 1 gradually catches up with soliton 2 and collides. Because soliton 1 is 'thin' and soliton 2 is 'fat', soliton 1 will be engulfed by soliton 2 when the collision occurred. After a while, when the collision

finished, soliton 1 is released from soliton 2 and restore its velocity and amplitude as before. However, soliton 2 is split into two fragments. Its waveform is completely damaged and unable to return to previous state. Thus, this collision is not a elastic collision.

4. Conclusion

A magnetized dusty plasma, which composed of low-temperature and high-temperature ions, electrons, and dust particles, is considered. The dynamical behaviors can be described by a 3D ZKE. A type of completely localized solitary waves of ZKE are obtained analytically and approximately for the first time. This kind of solitary wave is also confirmed numerically by the Petviashvili method. Both the analytical and numerical results indicate that the amplitude of the localized wave is proportional to its velocity and inverse proportional to the nonlinear interaction strength. A finite difference scheme with second-order accuracy is presented to make the long-time nonlinear evolution of ZKE. The numerical results indicate that the localized solitons are always dynamically stable. Moreover, the collision between two solitary waves is investigated numerically. The results show that both elastic and inelastic collision exist when two localized solitary waves colliding.

Acknowledgments

Project supported by the National Natural Science Foundation of P. R. China (Grant Nos. 11565021, 11047010), the Scientific Research Foundation of Northwest Normal University (Grant Nos. NWNU-LKQN-16-3, NWNU2019KT232).

References

[1] Morfill G E, Tsytovich V N and Thomas H 2003 Complex plasmas: II. Elementary processes in complex plasmas *Plasma. Phys. Rep.* **9** 1–30
[2] Shukla P K and Mamun A A 2002 Introduction to dusty plasma physics *Plasma Phys. Control. Fusion* **44** 395
[3] Mendis D A, Hill J R, Houpis H L F and Whipple E C 1981 On the electrostatic charging of the cometary nucleus *Astrophys. J.* **1** 787–97
[4] Shukla P K and Tskhakaya D D 2001 Instability of dust ion-acoustic waves in a dusty plasma containing elongated and rotating charged dust grains *Phys. Plasmas* **9** 661
[5] Piel A and Melzer A 2002 Dusty plasmas-the state of understanding from an experimentalist's view *Adv. Space. Res.* **29** 1255–64
[6] Merlino R L and Goree J A 2004 Dusty plasmas in the laboratory, industry, and space *Phys. Today.* **57** 32–8
[7] Morfill G E and Ivlev A V 2009 Complex plasmas: an interdisciplinary research field *Rev. Mod. Phys.* **81** 1353–404
[8] Nefedov A P *et al* 2009 PKE-Nefedov: plasma crystal experiments on the international space station *New. J. Phys.* **5** 33
[9] Samsonov D, Zhdanov S K and Quinn R A 2004 Shock melting of a two-dimensional complex (dusty) plasma *Phys. Rev. Lett.* **92** 255004
[10] Xiao D L, Ma J X and Li Y F 2005 Dust-acoustic shock waves: effect of plasma density gradient *Phys. Plasmas* **12** 052314
[11] Pustylnik M Y *et al* 2016 Plasmakristall-4: new complex (dusty) plasma laboratory on board the international space station *Rev. Sci. Instrum.* **87** 093505
[12] Ding Z Y, Qiao K, Ernst N, Kong J, Chen M D, Matthews L S and Hyde T W 2019 Nonlinear mode coupling and internal resonance observed in a dusty plasma *New J. Phys.* **21** 103051
[13] Ding Z Y, Qiao K, Kong J, Matthews L S and Hyde T W 2019 Nonlinear response of vertical paired structure in complex plasma *Plasma Phys. Control. Fusion* **61** 055004
[14] Jaiswal S, Bandyopadhyay P and Sen A 2016 Experimental observation of precursor solitons in a flowing complex plasma *Phys. Rev.* E **93** 041201(R)
[15] Eliasson B and Shukla P K 2009 Nonlinear aspects of quantum plasma physics: nanoplasmonics and nanostructures in dense plasmas *Plasma Fusion Res.* **4** 032
[16] Abdikian A 2017 Modulational instability of ion-acoustic waves in magnetoplasma with pressure of relativistic electrons *Phys. Plasmas* **24** 052123
[17] Akbari-Moghanjoughi M and Shukla P K 2012 Theory for large-amplitude electrostatic ion shocks in quantum plasmas *Phys. Rev.* E **86** 066401
[18] Abdikian A and Ismaeel S 2017 Ion-acoustic rogue waves and breathers in relativistically degenerate electron–positron plasmas *Eur. Phys. J. Plus* **132** 368
[19] Bhatti M M and Lu D Q 2019 Analytical study of the head-on collision process between hydroelastic solitary waves in the presence of a uniform current *Symmetry* **11** 333
[20] Abdelsalam Sara I, Bhatti M M and Zeeshan A 2019 Metachronal propulsion of a magnetized particle-fluid suspension in a ciliated channel with heat and mass transfer *Phys. Scr.* **94** 115301
[21] Marin M, Vlase S, Ellahi R and Bhatti M M 2019 On the partition of energies for the backward in time problem of thermoelastic materials with a dipolar structure *Symmetry* **11** 863
[22] Kundu S K, Ghosh D K, Chatterjee P and Das B 2011 Shock waves in a dusty plasma with positive and negative dust, where electrons are superthermally distributed *Bulg. J. Phys.* **38** 409–19
[23] Seadawy A R 2015 Nonlinear wave solutions of the three-dimensional Zakharov–Kuznetsov–Burgers equation in dusty plasma *Phys.* A **439** 124–31
[24] Shukla P K, Eliasson B and Sandberg I 2003 Theory of cavitons in complex plasmas *Phys. Rev. Lett.* **91** 075005
[25] Shukla P K and Silin V P 1992 Dust ion-acoustic wave *Phys. Scr.* **45** 508
[26] Verheest F, Shukla P K, Rao N N and Meuris P 1997 Dust-acoustic waves in self-gravitating dusty plasmas with fluctuating dust charges *J. Plasma Phys.* **58** 163–70
[27] Liu Z M, Duan W S and He G J 2008 Effects of dust size distribution on dust acoustic waves in magnetized two-ion-temperature dusty plasmas *Phys. Plasmas* **15** 083702
[28] Seadawy A R 2014 Stability analysis for Zakharov–Kuznetsov equation of weakly nonlinear ion-acoustic waves in a plasma *Comput. Math. Appl.* **67** 172–80
[29] Liu C B, Wang L X, Yang X and Shi Y R 2015 Transverse instability of dust-acoustic solitary waves in magnetized dusty plasmas *Plasma Sci. Technol.* **17** 298
[30] Duan W S, Hong X R, Shi Y R, Lu K P and Sun J A 2002 Weakly two-dimensional solitary waves on coupled nonlinear transmission lines *Chin. Phys. Lett.* **19** 1231

[31] Thomas E J, Merlino R L and Rosenberg M 2012 Magnetized dusty plasmas: the next frontier for complex plasma research *Plasma Phys. Control. Fusion* **54** 124034

[32] Bernhardt P A, Baumgardner J B, Bhatt A N, Erickson P J, Larsen M F and Pedersen T R 2011 Optical emissions observed during the charged aerosol release experiment (CARE I) in the ionosphere *IEEE. Trans. Plasma. Sci.* **39** 2774–5

[33] Chow V W, Mendis D A and Rosenberg M 1993 Role of grain size and particle velocity distribution in secondary electron emission in space plasmas *J. Geophys. Res. Space* **98** 19065–76

[34] Álvarez J and Durán A 2014 *J. Comput. Appl. Math.* **266** 39–51

[35] Álvarez J and Durán A 2014 An extended Petviashvili method for the numerical generation of traveling and localized waves *Commun. Nonlinear. Sci.* **19** 2272–83

[36] Yang J K 2010 *Nonlinear Waves in Integrable and Nonintegrable Systems* (Philadelphia: SIAM) pp 269–83 978-0-89871-705-1

[37] Lu J F and Guan Z 2003 *Numerical Methods for Solving Partial Differential Equations* (Beijing: Tsinghua University Press) pp 155–7 (in Chinese)